OSUG

Observatoire des Sciences de l'Univers de Grenoble

Climate change in the High Mountain Asia simulated with CMIP6 models

Mickaël Lalande

PhD Student 2019-2022
Supervisors : Martin Ménégoz and Gerhard Krinner

Institut des Géosciences de l'Environnement (IGE, Grenoble, France)

Réunion chantier Himalaya — 29/03/2021

1. Introduction
2. Data and methods
3. Historical bias analysis
4. Projections
5. Discussion / Conclusion

1. Introduction

High Mountain Asia (HMA): Introduction

- The Tibetan Plateau (TP) region is the world’s highest plateau (average elevation 4000m) ➝ considerable influence on regional and global climate. (e.g., Kutzbach et al., 1993)
- Directly sustain the livelihoods of 240 million people in the mountain and hills of the Hindu Kush Himalaya. (Sharma et al., 2019)
- Two distinct climatic regimes:
  - winter westerly disturbances (WDs) ➝ 50 % of the precipitation over the western Himalaya and Hindu Kush mountains
  - central and eastern Himalayan mountains receiving major part (up to 80%) of annual precipitation during the Indian summer monsoon months (June-September). (Bookhagen and Burbank, 2010)

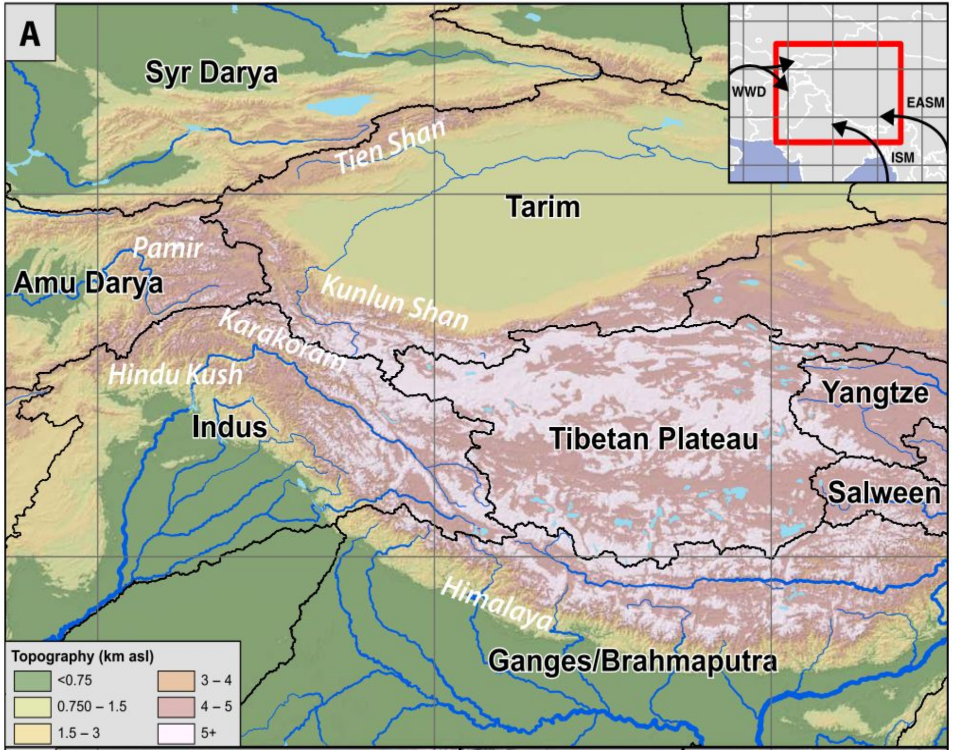

Smith and Bookhagen (2018), Fig. 1A

Changes over HMA

- TP experienced a more pronounced warming than the regions located at the same latitude (Rangwala et al., 2013)
- Warming over the TP of 0.16 °C/dec (0.32 °C/dec in winter) over 1955-1996 (Liu et al., 2000) and 0.36 °C/dec over 1960-2007 (Wang et al., 2008)
- Precipitation and snow cover show contrasted trends over the TP (Kang et al., 2010).
- Climate change in HMA and TP affects: permafrost (Yang et al., 2010), glaciers (Yao et al., 2007), desertification (Xue et al., 2009), water resources (e.g. Immerzeel et al., 2010), etc.
- Lack of observations: western part and high elevation
  -> limits the possibility to understand and to anticipate the climate change in this area

Use of GCMs (even if coarse spatial resolution ~50-300km) provides a coherent picture of the large-scale temporal and spatial patterns of key variables at a regional scale !

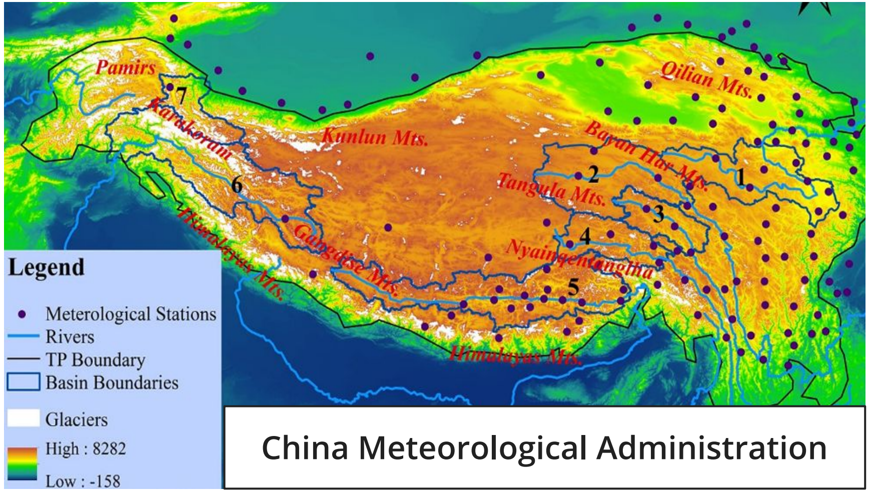

Li et al. (2018), Fig. 1

“Cold bias” over Tibetan Plateau

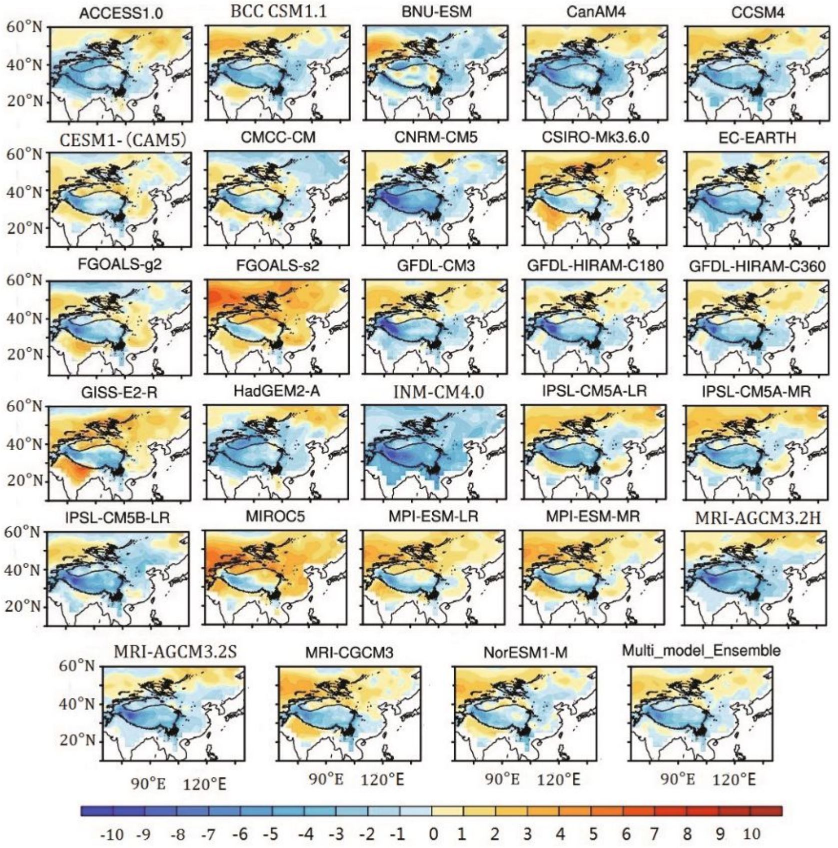

Fig. 2. Annual mean T_{as} (°C) differences between various models and CRU data averaged during 1979–2005. All air temperature values in the models have been corrected to real elevation at a resolution of 2.5° × 2.5°.

- Cold biases in models from first AMIP experiments (Mao and Robock, 1998)
- Still present in CMIP5 and CMIP6 (Chen et al., 2017; Salunke et al., 2019)
- Possible explanations:
  - Excess precipitation in these regions (Lee & Suh, 2000)
  - deficiency in the representation of snow–ice albedo in models (Su et al., 2013)
  - Cold biases also observed in T500 -> dry and cold air from the deserts of western Asia due to an smoothed topography ? (Boos and Hurley, 2013)
  - Improvements in the parameterization of the area of snow cover, as well as the boundary layer, and hence surface turbulent fluxes, may help to reduce the cold bias over the TP in the models. (Chen et al., 2017)
  - \+ lack of high-elevation observation stations in the CRU (Gu et al., 2012)
- **Our study:**

1. Are the biases in HMA still present in the new generation of climate models for near-surface air temperature (tas), total precipitation (pr), and snow cover extent (snc)?
2. What are the links between the model biases in tas, pr, and snc?
3. Do the model biases impact the simulated climate trends?
4. Which climate projections can be expected in this area over the next century?

2. Data and methods

Data and methods

- 26 GCMs from CMIP6 (Eyring et al., 2016) simulations for historical period 1979-2014
- 10 CMIP6 models for the future projections: SSP1-2.6, SSP2-4.5, SSP3-7.0 and SSP5-8.5 (O'Neill et al., 2016)
- Variables: Near-Surface Air Temperature (tas), Snow Cover Extent (snc) and Total Precipitation (pr)
- Observations:
  - tas: CRU TS (Climatic Research Unit gridded Time Series) version 4.00 (http://doi.org/10/gbr3nj)
  - snc: NOAA Climate Data Record (CDR) of Northern Hemisphere (NH) Snow Cover Extent (SCE), Version 1 (Robinson et al., 2012; satellite weekly binary product)
  - pr (undercatch solid precipitations):
    - APHRODITE version V1101 (1951 - 2007) and V1101EX_R1 (2007 - 2015) (Yatagai et al., 2012)
    - Global Precipitation Climatology Project (GPCP) Climate Data Record (CDR), Version 2.3 (Monthly) product at 2.5° (Adler et al., 2016)
  - Topography: Global Multi-resolution Terrain Elevation Data 2010 (GMTED2010) (https://www.temis.nl/data/gmted2010/index.php)
- Reanalyses: ERA-Interim (Dee et al., 2011) and ERA5 (Hersbach et al., 2020)

Zone of study

- High Mountain of Asia (HMA) box covering 60E° - 110°E and 20N° - 45°N including the Tibetan Plateau (TP), with elevation higher than 2500 m.asl (red contour)

- 3 subdomains (> 2500 m.asl):
  - Hindu-Kush Karakoram (HK): 70° - 81°E; 31° - 40°N
  - Himalaya (HM): 79° - 98°E; 26° - 31°N)
  - Tibetan Plateau (TP): 81° - 104°E; 31° - 39°N

- Seasons:
  - Winter: DJFMA (WDs)
  - Summer: JJAS (Asian summer monsoon)

Annual climatologies computed over 1979-2014 of observations (c,e,g) and the multimodel mean (d,f,h; first realization of each ensemble model).

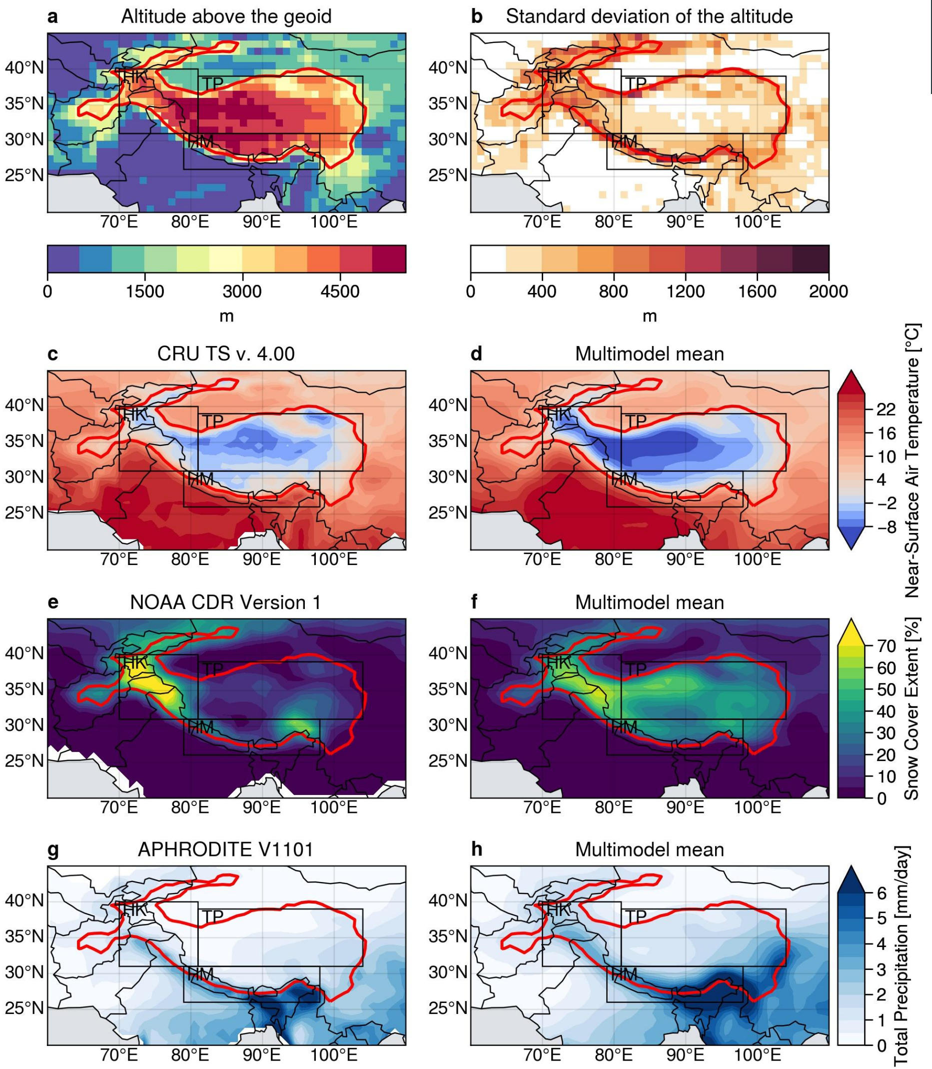

3. Historical bias analysis

tas, snc and pr annual cycles

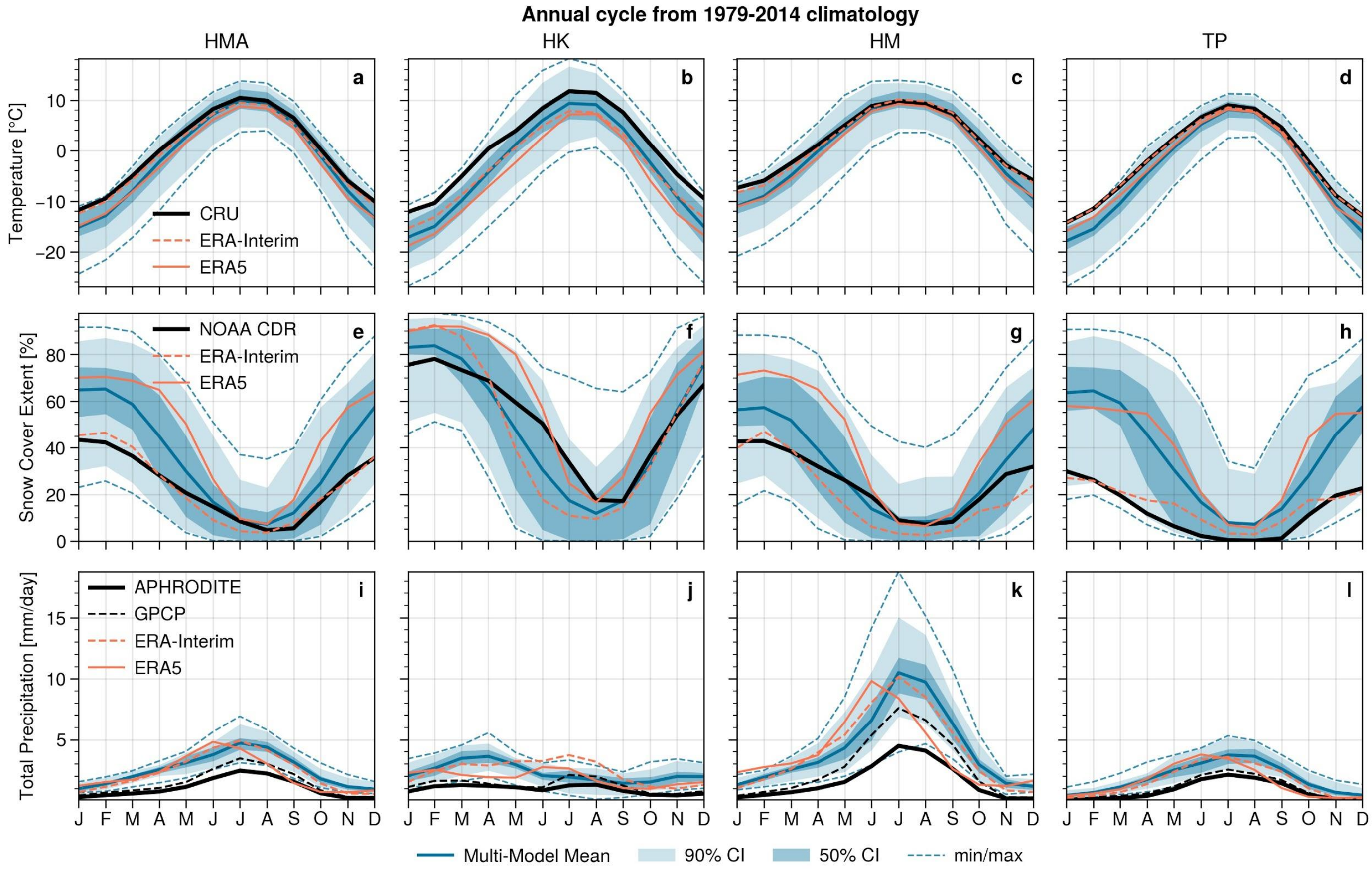

- stronger biases in winter for tas (~2/3°C) and snc (~20%) over HMA
- large snc spread -> difficulty to simulate snc in complex topography areas
- ERA5 bias similar to models
  -> does not assimilate IMS data beyond 1500 meters altitude (Orsolini et al., 2019)
  -> single-layer snow scheme does not allow enough melting in mountainous regions (Hersbach et al., 2020)
- pr obs lower than models
  -> snow undercatch issues by rain gauge (e.g. Jimeno-Saez et al., 2020)

Spatial biases and metrics

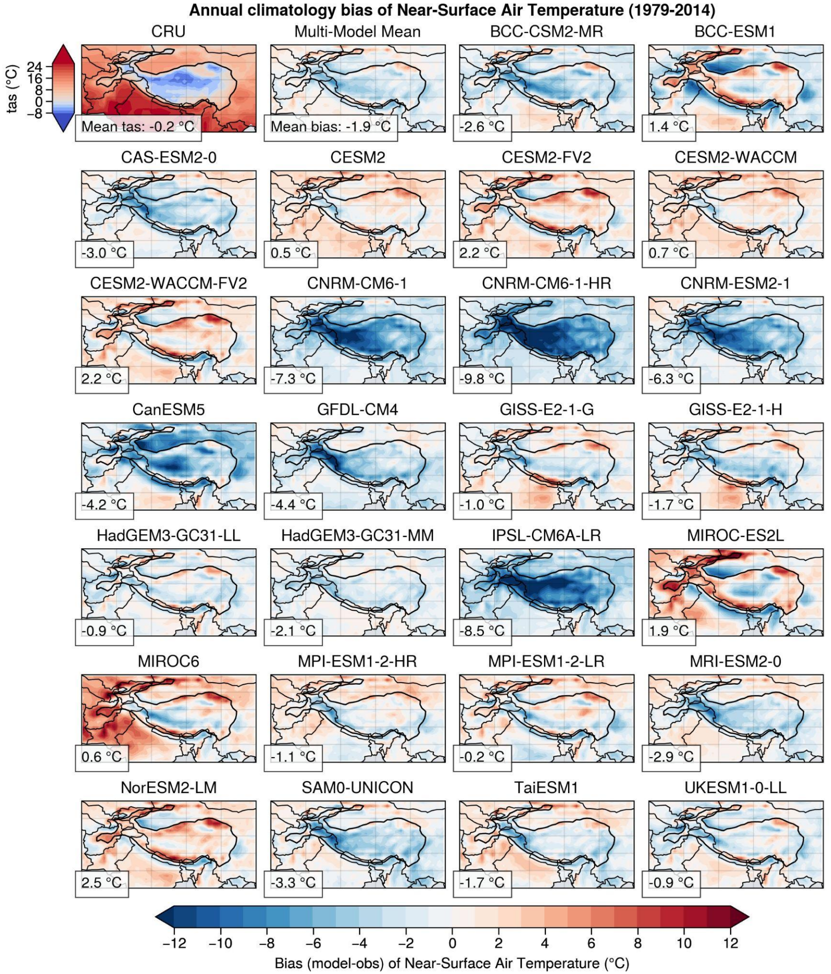

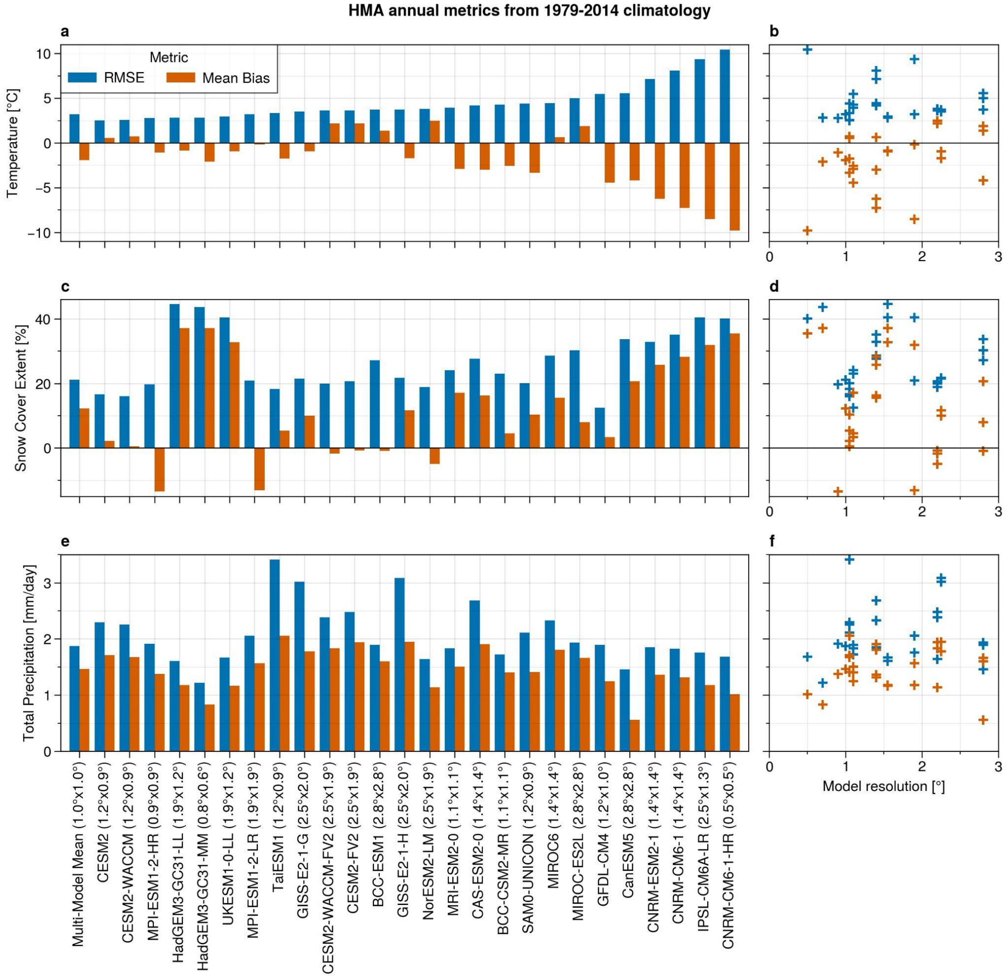

Bias spatial correlation

Annual spatial correlation of bias over HMA from 1979-2014 climatology

	BCC-CSM2-MR	BCC-ESM1	CAS-ESM2-0	CESM2	CESM2-FV2	CESM2-WACCM	CESM2-WACCM-FV2	CNRM-CM6-1	CNRM-CM6-1-HR	CNRM-ESM2-1	CanESM5	GFDL-CM4	GISS-E2-1-G	GISS-E2-1-H	HadGEM3-GC31-LL	HadGEM3-GC31-MM	IPSL-CM6A-LR	MIROC-ES2L	MIROC6	MPI-ESM1-2-HR	MPI-ESM1-2-LR	MRI-ESM2-0	NorESM2-LM	SAM0-UNICON	TaiESM1	UKESM1-0-LL
tas normalized bias	−0.26	0.14	−0.31	0.06	0.22	0.07	0.22	−0.74	−1	−0.64	−0.43	−0.45	−0.1	−0.18	−0.09	−0.21	−0.87	0.19	0.07	−0.11	−0.02	−0.3	0.25	−0.34	−0.2	−0.1
tas bias / snc bias	**-0.51**	**-0.45**	**-0.21**	−0.02	**-0.29**	0.01	**-0.29**	**-0.5**	**-0.39**	**-0.47**	**-0.53**	**-0.4**	**-0.36**	**-0.35**	**-0.28**	**0.16**	**-0.62**	**-0.71**	**-0.58**	0.09	**-0.23**	**-0.16**	**-0.25**	**-0.18**	−0.09	**-0.17**
tas bias / pr bias	−0.09	**-0.22**	−0.08	**-0.18**	**-0.21**	**-0.19**	**-0.22**	0.02	−0.05	−0.02	**0.16**	**-0.16**	**-0.11**	−0.04	−0.04	−0.07	0.02	−0.07	0.02	**-0.37**	**-0.35**	**-0.24**	**-0.26**	**-0.12**	**-0.14**	−0.02
snc bias / pr bias	**0.18**	**0.48**	**0.41**	**-0.22**	−0.05	**-0.18**	−0.04	**-0.23**	**-0.38**	**-0.23**	−0.06	0.04	−0.02	0.03	0.05	−0.04	0.06	0.01	**-0.31**	**-0.12**	0.1	**-0.22**	**0.13**	0.1	0.01	−0.03
tas bias / elevation	**-0.41**	−0.04	**-0.36**	**-0.28**	−0.09	**-0.26**	−0.1	**-0.56**	**-0.66**	**-0.55**	**-0.32**	**-0.37**	**-0.34**	**-0.43**	**-0.16**	−0.09	**-0.63**	**-0.28**	**-0.52**	**-0.3**	**-0.21**	**-0.42**	−0.05	**-0.45**	**-0.34**	**-0.12**
snc bias / elevation	**0.63**	**0.5**	**0.5**	**0.53**	**0.46**	**0.51**	**0.44**	**0.54**	**0.67**	**0.53**	**0.5**	**0.45**	**0.46**	**0.5**	**0.47**	**0.32**	**0.56**	**0.41**	**0.56**	**0.22**	**0.24**	**0.44**	**0.29**	**0.48**	**0.39**	**0.49**
pr bias / elevation	**0.18**	**0.43**	**0.12**	**-0.13**	0.07	**-0.12**	0.07	**-0.15**	**-0.31**	**-0.13**	−0.05	−0.08	**-0.19**	**-0.18**	0.01	**-0.28**	−0.06	0.03	−0.05	−0.01	**0.15**	0.01	−0.01	−0.03	**-0.12**	0.01

- Significant negative correlations between tas and snc biases
- Less obvious for pr (/!\ APHRODITE underestimate solid precip /!\ -> more negative correlation)
- Correlations between tas/snc biases with elevation -> difficulty representing physical processes at high elevation?

Are trends impacted by overall biases?

Historical trends analysis

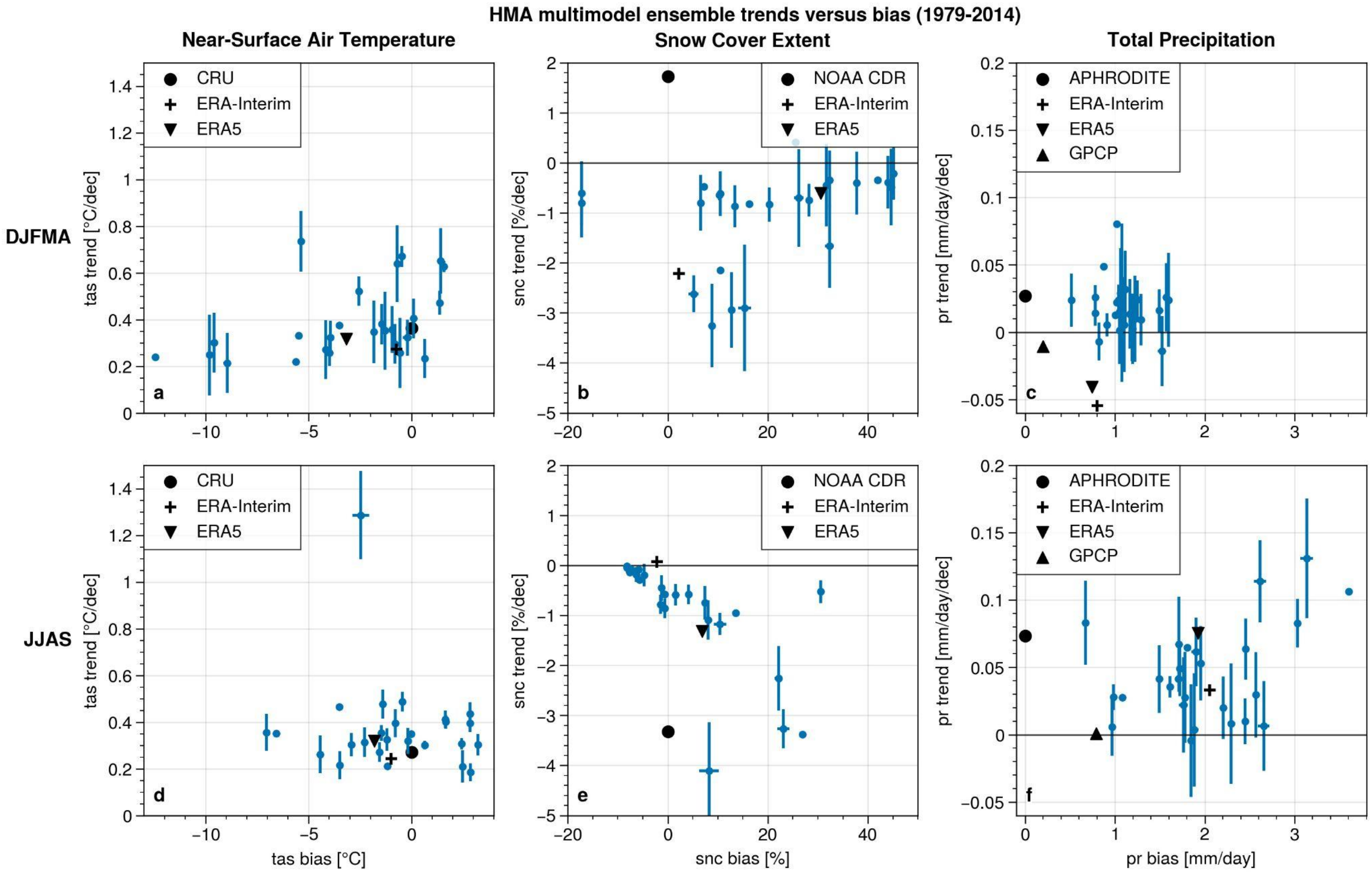

- No obvious link between model biases and trends
- Some strongly biased models have trends close to observations
- On the contrary, some models with little bias have very different trends
- Except for snow cover in summer -> very small snow cover

-> All available models are kept for projections

4. Projections

Projections

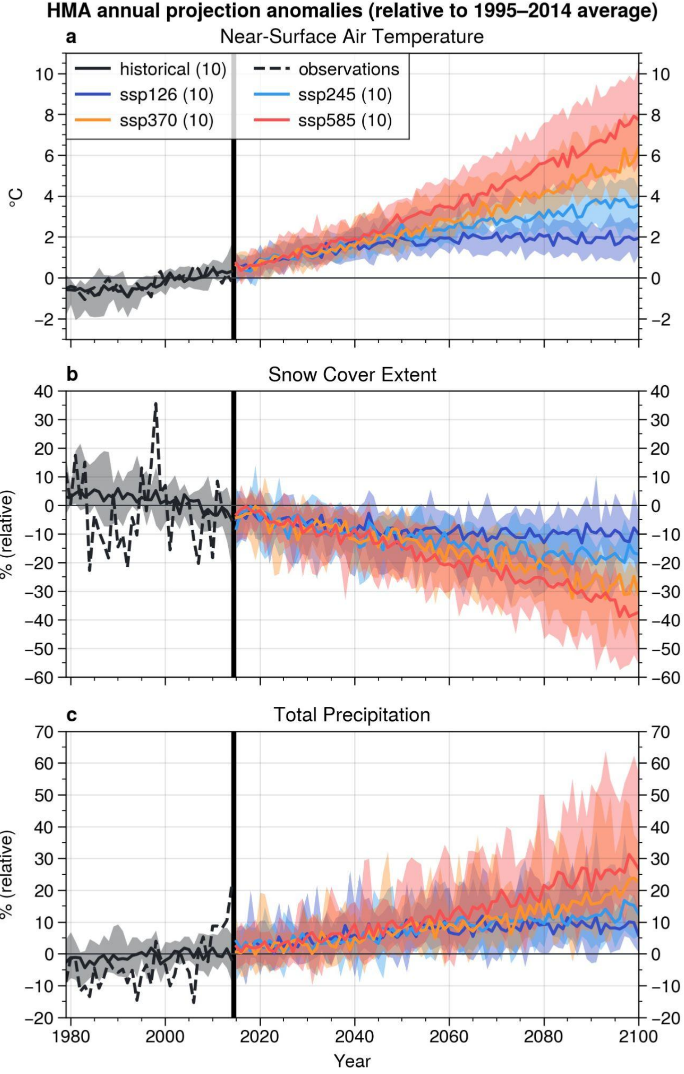

- 2081-2100 with respect to 1995-2014 average:
  - tas: 1.9 [1.2 to 2.7] °C (SSP1-2.6) to 6.5 [4.9 to 9.0] °C (SSP5-8.5)
  - snc: -9.4 [-16.4 to -5.0] % (SSP1-2.6) to -32.2 [-49.1 to -25.0] % (SSP5-8.5)
  - pr: 8.5 [4.8 to 18.2] % (SSP1-2.6) to 24.9 [14.4 to 48.1] % (SSP5-8.5)

- snc and pr models variability underestimated?

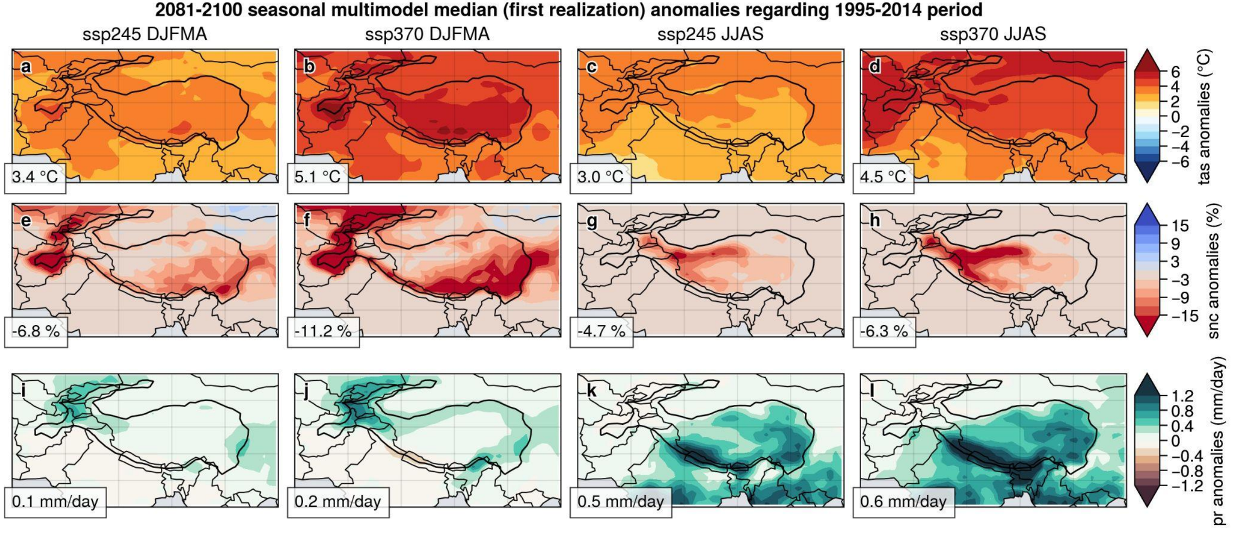

HMA versus global

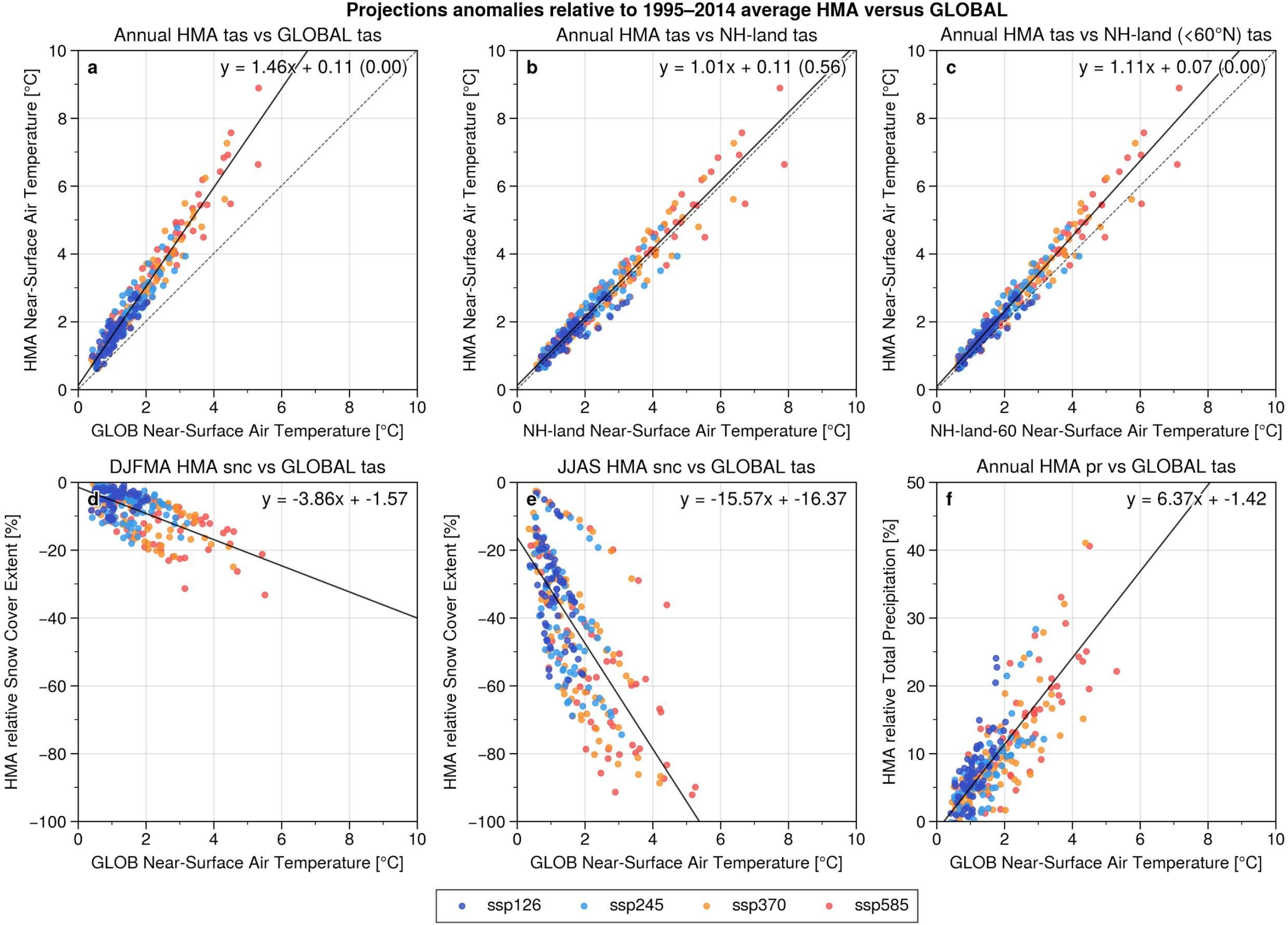

- HMA is warming faster as the rest of the world ?
- 1.1 faster… compared to NH (without Arctic)
- ~ 4% relative snc loss per 1°C GSAT in winter (linear)
- In summer almost all snc disappear in worst scenario (not linear)
- ~ 6 % relative more pr per 1°C GSAT

5. Discussion / Conclusion

Discussion / Conclusion

- 26 CMIP6 GCMs to simulate:
    - Near-Surface Air Temperature (tas) / Snow Cover Extent (snc) / Total Precipitation (pr)
- Period: 1979-2014 and projected changes (for 10 of them)
- Zone: High Mountain of Asia (HMA) region (including TP)

- Biases still present in CMIP6 models over HMA (more pronounced in winter for tas and snc) annual:
    - tas: cold bias of -1.9 [-8.2 to 2.9] °C
    - snc overestimated 12 [-13 to 43] % (or 52 [-53 to 183] % relative)
    - pr overestimated 1.5 [0.3 to 2.9] mm.day-1 (or 143 [31 to 281] % relative) /!\ obs /!\

- No obvious link between biases and trends -> biased models seems able to reproduce past trends
- Models resolution doesn't seem to be a "magic" solution! Additional improvements in parameterizations seems essential!

Discussion / Conclusion

- The bias seems to have different origin from one model to another (precipitation, snow cover, elevation, etc.)
- Other variables might be involved! (cloud cover, aerosols, boundary layer, T500, etc.)

Usha et al. (2020), Fig. 7

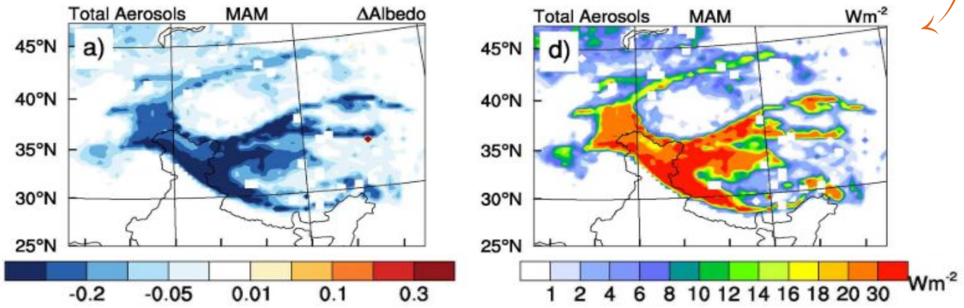

DeWekker et al. (2015); Serafin et al. (2020)

"limited applicability of existing turbulence theory with frequent violation of its basic assumptions (e.g., stationarity and isotropy of small-scale turbulence) over mountainous areas"

- The origin of the bias seems complex to determine in this region and must be the result of many factors, in addition that observations are far from perfect...

Future work

Implementation of a snow cover parameterization taking into account the variation of subgrid topography in LMDZ

Bibliography

References

Abramowitz, M., & Irene, S. (1964). Handbook of Mathematical Functions, pp. 931-995. Retrieved from http://people.math.sfu.ca/~cbm/aands/abramowitz_and_stegun.pdf

Adler, Robert; Wang, Jian-Jian; Sapiano, Matthew; Huffman, George; Chiu, Long; Xie, Ping Ping; Ferraro, Ralph; Schneider, Udo; Becker, Andreas; Bolvin, David; Nelkin, Eric; Gu, Guojun; and NOAA CDR Program (2016). Global Precipitation Climatology Project (GPCP) Climate Data Record (CDR), Version 2.3 (Monthly). National Centers for Environmental Information. https://doi.org/10.7289/V56971M6

Bookhagen, B., & Burbank, D. W. (2010). Toward a complete Himalayan hydrological budget: Spatiotemporal distribution of snowmelt and rainfall and their impact on river discharge. Journal of Geophysical Research: Earth Surface, 115(3), 1–25. https://doi.org/10.1029/2009JF001426

Boos, W. R., & Hurley, J. V. (2013). Thermodynamic bias in the multimodel mean boreal summer monsoon. Journal of Climate, 26(7), 2279–2287. https://doi.org/10.1175/JCLI-D-12-00493.1

Chen, X., Liu, Y., & Wu, G. (2017). Understanding the surface temperature cold bias in CMIP5 AGCMs over the Tibetan Plateau. Advances in Atmospheric Sciences, 34(12), 1447–1460. https://doi.org/10.1007/s00376-017-6326-9

Dee, D. P., Uppala, S. M., Simmons, A. J., Berrisford, P., Poli, P., Kobayashi, S., ... Vitart, F. (2011). The ERA-Interim reanalysis: configuration and performance of the data assimilation system. Quarterly Journal of the Royal Meteorological Society, 137(656), 553–597. https://doi.org/10.1002/qj.828

Deser, C., Terray, L., & Phillips, A. S. (2016). Forced and internal components of winter air temperature trends over North America during the past 50 years: Mechanisms and implications. Journal of Climate, 29(6), 2237–2258. https://doi.org/10.1175/JCLI-D-15-0304.1

References

De Wekker, S. F. J., & Kossmann, M. (2015). Convective Boundary Layer Heights Over Mountainous Terrain—A Review of Concepts. Frontiers in Earth Science, 3(December), 1–22. https://doi.org/10.3389/feart.2015.00077

Eyring, V., Bony, S., Meehl, G. A., Senior, C. A., Stevens, B., Stouffer, R. J., & Taylor, K. E. (2016). Overview of the Coupled Model Intercomparison Project Phase 6 (CMIP6) experimental design and organization. Geoscientific Model Development, 9(5), 1937–1958. https://doi.org/10.5194/gmd-9-1937-2016

Gu, H., Wang, G., Yu, Z., & Mei, R. (2012). Assessing future climate changes and extreme indicators in east and south Asia using the RegCM4 regional climate model. Climatic Change, 114(2), 301–317. https://doi.org/10.1007/s10584-012-0411-y

Hersbach, H., Bell, B., Berrisford, P., Hirahara, S., Horányi, A., Muñoz-Sabater, J., … Thépaut, J. (2020). The ERA5 global reanalysis. Quarterly Journal of the Royal Meteorological Society, 146(730), 1999–2049. https://doi.org/10.1002/qj.3803

Immerzeel, W. W., van Beek, L. P. H., & Bierkens, M. F. P. (2010). Climate Change Will Affect the Asian Water Towers. Science, 328(5984), 1382–1385. https://doi.org/10.1126/science.1183188

Immerzeel, W. W., Wanders, N., Lutz, A. F., Shea, J. M., & Bierkens, M. F. P. (2015). Reconciling high-altitude precipitation in the upper Indus basin with glacier mass balances and runoff. Hydrology and Earth System Sciences, 19(11), 4673–4687. https://doi.org/10.5194/hess-19-4673-2015

Jimeno-Sáez, P., Pulido-Velazquez, D., Collados-Lara, A.-J., Pardo-Igúzquiza, E., Senent-Aparicio, J., & Baena-Ruiz, L. (2020). A Preliminary Assessment of the "Undercatching" and the Precipitation Pattern in an Alpine Basin. Water, 12(4), 1061. https://doi.org/10.3390/w12041061

Kang, S., Xu, Y., You, Q., Flügel, W.-A., Pepin, N., & Yao, T. (2010). Review of climate and cryospheric change in the Tibetan Plateau. Environmental Research Letters, 5(1), 015101. https://doi.org/10.1088/1748-9326/5/1/015101

References

Kutzbach, J. E., Prell, W. L., & Ruddiman, W. F. (1993). Sensitivity of Eurasian Climate to Surface Uplift of the Tibetan Plateau. The Journal of Geology, 101(2), 177–190. https://doi.org/10.1086/648215

Lee, D. K., & Suh, M. S. (2000). Ten-year east Asian summer monsoon simulation using a regional climate model (RegCM2). Journal of Geophysical Research Atmospheres, 105(D24), 29565–29577. https://doi.org/10.1029/2000JD900438

Li, C., Su, F., Yang, D., Tong, K., Meng, F., & Kan, B. (2018). Spatiotemporal variation of snow cover over the Tibetan Plateau based on MODIS snow product, 2001-2014. International Journal of Climatology, 38(2), 708–728. https://doi.org/10.1002/joc.5204

Liu, X., & Chen, B. (2000). Climatic warming in the Tibetan Plateau during recent decades. International Journal of Climatology, 20(14), 1729–1742. https://doi.org/10.1002/1097-0088(20001130)20:14<1729::AID-JOC556>3.0.CO;2-Y

Mao, J., & Robock, A. (1998). Surface Air Temperature Simulations by AMIP General Circulation Models: Volcanic and ENSO Signals and Systematic Errors. Journal of Climate, 11(7), 1538–1552. https://doi.org/10.1175/1520-0442(1998)011<1538:SATSBA>2.0.CO;2

O'Neill, B. C., Tebaldi, C., van Vuuren, D. P., Eyring, V., Friedlingstein, P., Hurtt, G., ... Sanderson, B. M. (2016). The Scenario Model Intercomparison Project (ScenarioMIP) for CMIP6. Geoscientific Model Development, 9(9), 3461–3482. https://doi.org/10.5194/gmd-9-3461-2016

Orsolini, Y., Wegmann, M., Dutra, E., Liu, B., Balsamo, G., Yang, K., ... Arduini, G. (2019). Evaluation of snow depth and snow cover over the Tibetan Plateau in global reanalyses using in situ and satellite remote sensing observations. The Cryosphere, 13(8), 2221–2239. https://doi.org/10.5194/tc-13-2221-2019

Palazzi, E., von Hardenberg, J., & Provenzale, A. (2013). Precipitation in the Hindu-Kush Karakoram Himalaya: Observations and future scenarios. Journal of Geophysical Research: Atmospheres, 118(1), 85–100. https://doi.org/10.1029/2012JD018697

References

Robinson, David A.; Estilow, Thomas W.; and NOAA CDR Program (2012): NOAA Climate Data Record (CDR) of Northern Hemisphere (NH) Snow Cover Extent (SCE), Version 1. NOAA National Centers for Environmental Information. https://doi.org/10.7289/V5N014G9

Rangwala, I., Sinsky, E., & Miller, J. R. (2013). Amplified warming projections for high altitude regions of the northern hemisphere mid-latitudes from CMIP5 models. Environmental Research Letters, 8(2), 024040. https://doi.org/10.1088/1748-9326/8/2/024040

Salunke, P., Jain, S., & Mishra, S. K. (2019). Performance of the CMIP5 models in the simulation of the Himalaya-Tibetan Plateau monsoon. Theoretical and Applied Climatology, 137(1–2), 909–928. https://doi.org/10.1007/s00704-018-2644-9

Serafin, S., Rotach, M. W., Arpagaus, M., Colfescu, I., Cuxart, J., De Wekker, S. F. J., … Zardi, D. (2020). Multi-scale transport and exchange processes in the atmosphere over mountains. In Multi-scale transport and exchange processes in the atmosphere over mountains. https://doi.org/10.15203/99106-003-1

Sharma, E., Molden, D., Rahman, A., Khatiwada, Y. R., Zhang, L., Singh, S. P., … Wester, P. (2019). Introduction to the Hindu Kush Himalaya Assessment. In The Hindu Kush Himalaya Assessment (pp. 1–16). https://doi.org/10.1007/978-3-319-92288-1_1

Smith, T., & Bookhagen, B. (2018). Changes in seasonal snow water equivalent distribution in High Mountain Asia (1987 to 2009). *Science Advances*, *4*(1), e1701550. https://doi.org/10.1126/sciadv.1701550

Su, F., Duan, X., Chen, D., Hao, Z., & Cuo, L. (2013). Evaluation of the Global Climate Models in the CMIP5 over the Tibetan Plateau. Journal of Climate, 26(10), 3187–3208. https://doi.org/10.1175/JCLI-D-12-00321.1

Usha, K. H., Nair, V. S., & Babu, S. S. (2020). Modeling of aerosol induced snow albedo feedbacks over the Himalayas and its implications on regional climate. Climate Dynamics, (0123456789). https://doi.org/10.1007/s00382-020-05222-5

References

Wang, B., Bao, Q., Hoskins, B., Wu, G., & Liu, Y. (2008). Tibetan Plateau warming and precipitation changes in East Asia. Geophysical Research Letters, 35(14), L14702. https://doi.org/10.1029/2008GL034330

Wang, X., Yang, M., Wan, G., Chen, X., & Pang, G. (2013). Qinghai-Xizang (Tibetan) Plateau climate simulation using the regional climate model RegCM3. Climate Research, 57(3), 173–186. https://doi.org/10.3354/cr01167

Xu, J., Gao, Y., Chen, D., Xiao, L., & Ou, T. (2017). Evaluation of global climate models for downscaling applications centred over the Tibetan Plateau. International Journal of Climatology, 37(2), 657–671. https://doi.org/10.1002/joc.4731

Xue, X., Guo, J., Han, B., Sun, Q., & Liu, L. (2009). The effect of climate warming and permafrost thaw on desertification in the Qinghai–Tibetan Plateau. Geomorphology, 108(3–4), 182–190. https://doi.org/10.1016/j.geomorph.2009.01.004

Yang, M., Nelson, F. E., Shiklomanov, N. I., Guo, D., & Wan, G. (2010). Permafrost degradation and its environmental effects on the Tibetan Plateau: A review of recent research. Earth-Science Reviews, 103(1–2), 31–44. https://doi.org/10.1016/j.earscirev.2010.07.002

Yao, T., Pu, J., Lu, A., Wang, Y., & Yu, W. (2007). Recent glacial retreat and its impact on hydrological processes on the Tibetan Plateau, China, and surrounding regions. Arctic, Antarctic, and Alpine Research, 39(4), 642–650. https://doi.org/https://doi.org/10.1657/1523-0430(07-510)[YAO]2.0.CO;2

Yao, T., Thompson, L., Yang, W., Yu, W., Gao, Y., Guo, X., ... Joswiak, D. (2012). Different glacier status with atmospheric circulations in Tibetan Plateau and surroundings. Nature Climate Change, 2(9), 663–667. https://doi.org/10.1038/nclimate1580

Yatagai, A., Kamiguchi, K., Arakawa, O., Hamada, A., Yasutomi, N., & Kitoh, A. (2012). APHRODITE: Constructing a Long-Term Daily Gridded Precipitation Dataset for Asia Based on a Dense Network of Rain Gauges. Bulletin of the American Meteorological Society, 93(9), 1401–1415. https://doi.org/10.1175/BAMS-D-11-00122.1

Supplementary materials

CMIP6 models

CMIP6 institute	CMIP6 model	Resolution (lonxlat)	Grid	Calendar	Member	SSP
BCC	BCC-CSM2-MR	1.1°x1.1°	gn	365_day	r1i1p1f1	
	BCC-ESM1	2.8°x2.8°				
CAS	CAS-ESM2-0	1.4°x1.4°	gn	365_day	r4i1p1f1	
NCAR	CESM2	1.2°x0.9°	gn	noleap	r1i1p1f1	
	CESM2-FV2	2.5°x1.9°				
	CESM2-WACCM	1.2°x0.9°				
	CESM2-WACCM-FV2	2.5°x1.9°				
CNRM-CERFACS	CNRM-CM6-1	1.4°x1.4°	gr	gregorian	r1i1p1f2	
	CNRM-CM6-1-HR	0.5°x0.5°				
	CNRM-ESM2-1	1.4°x1.4°				
CCCma	CanESM5	2.8°x2.8°	gn	365_day	r3i1p2f1	
NOAA-GFDL	GFDL-CM4	1.2°x1.0°	gr1	noleap	r1i1p1f1	
NASA-GISS	GISS-E2-1-G	2.5°x2.0°	gn	365_day	r1i1p1f1	
	GISS-E2-1-H					
MOHC	HadGEM3-GC31-LL	1.9°x1.2°	gn	360_day	r1i1p1f3	
	HadGEM3-GC31-MM	0.8°x0.6°				
IPSL	IPSL-CM6A-LR	2.5°x1.3°	gr	gregorian	r1i1p1f1	
MIROC	MIROC-ES2L	2.8°x2.8°	gn	gregorian	r1i1p1f2	
	MIROC6	1.4°x1.4°			r1i1p1f1	
MPI-M	MPI-ESM1-2-HR	0.9°x0.9°	gn	proleptic_gregorian	r1i1p1f1	
	MPI-ESM1-2-LR	1.9°x1.9°				
MRI	MRI-ESM2-0	1.1°x1.1°	gn	proleptic_gregorian	r1i1p1f1	
NCC	NorESM2-LM	2.5°x1.9°	gn	noleap	r2i1p1f1	
SNU	SAM0-UNICON	1.2°x0.9°	gn	noleap	r1i1p1f1	
AS-RCEC	TaiESM1	1.2°x0.9°	gn	noleap	r1i1p1f1	
MOHC, NIMS-KMA	UKESM1-0-LL	1.9°x1.2°	gn	360_day	r1i1p1f2	

Historical bias analysis

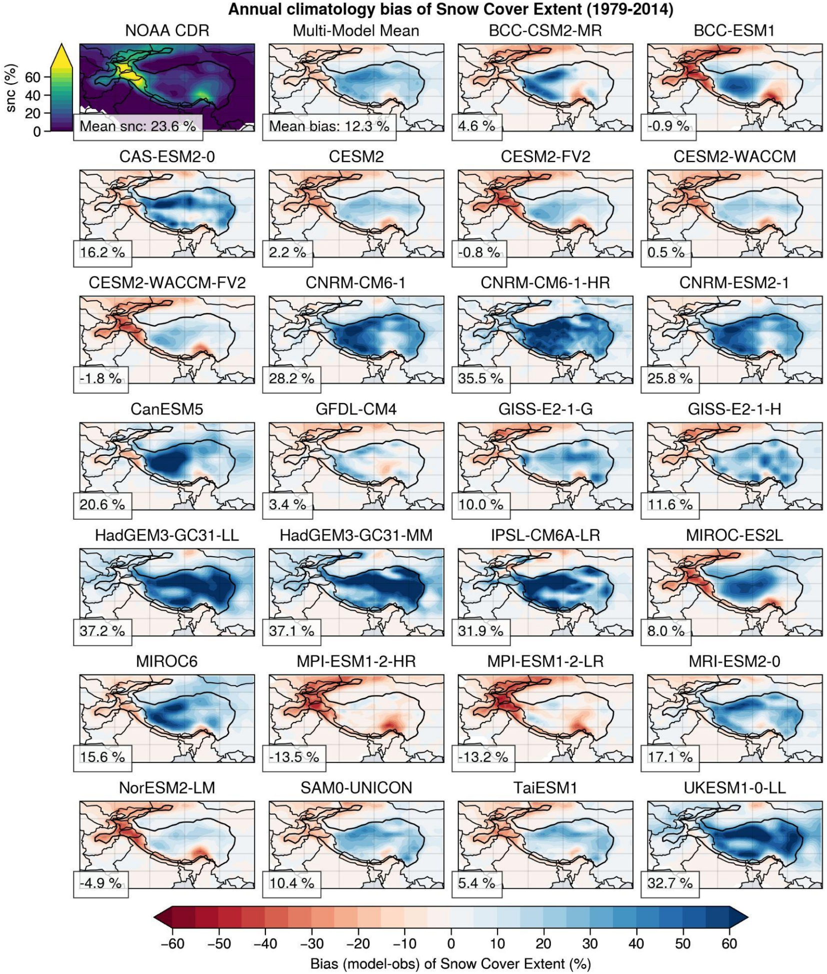

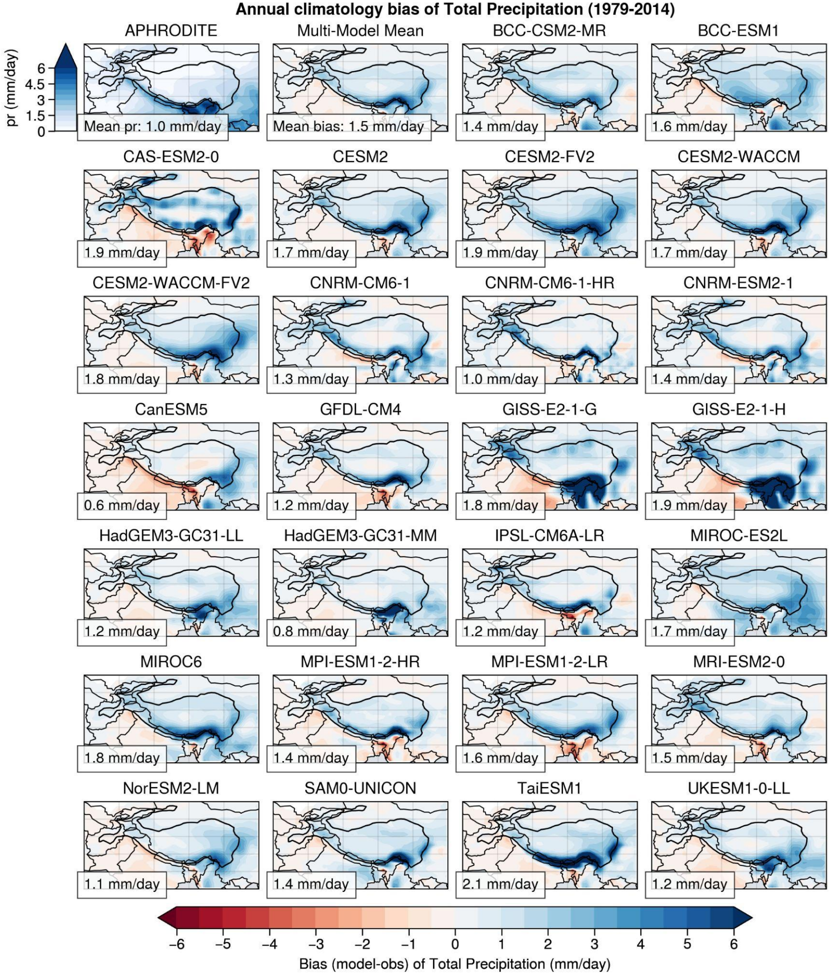

Bias spatial correlation (GPCP)

Annual spatial correlation of bias over HMA from 1979-2014 climatology

	BCC-CSM2-MR	BCC-ESM1	CAS-ESM2-0	CESM2	CESM2-FV2	CESM2-WACCM	CESM2-WACCM-FV2	CNRM-CM6-1	CNRM-CM6-1-HR	CNRM-ESM2-1	CanESM5	GFDL-CM4	GISS-E2-1-G
tas normalized bias	−0.26	0.14	−0.31	0.06	0.22	0.07	0.22	−0.74	−1	−0.64	−0.43	−0.45	−0.1
tas bias / snc bias	−0.51	−0.45	−0.21	−0.02	−0.29	0.01	−0.29	−0.5	−0.39	−0.47	−0.53	−0.4	−0.36
tas bias / pr bias	−0.03	−0.33	−0.02	−0.08	−0.2	−0.08	−0.21	0.1	0.02	0.07	0.15	−0.05	−0.07
snc bias / pr bias	0.21	0.7	0.45	−0.22	−0.02	−0.18	−0.01	−0.26	−0.36	−0.25	0	−0.05	−0.01
tas bias / elevation	−0.41	−0.04	−0.36	−0.28	−0.09	−0.26	−0.1	−0.56	−0.66	−0.55	−0.32	−0.37	−0.34
snc bias / elevation	0.63	0.5	0.5	0.53	0.46	0.51	0.44	0.54	0.67	0.53	0.5	0.45	0.46
pr bias / elevation	0.05	0.37	0.05	−0.27	−0.03	−0.26	−0.04	−0.32	−0.44	−0.3	−0.18	−0.24	−0.28

	GISS-E2-1-H	HadGEM3-GC31-LL	HadGEM3-GC31-MM	IPSL-CM6A-LR	MIROC-ES2L	MIROC6	MPI-ESM1-2-HR	MPI-ESM1-2-LR	MRI-ESM2-0	NorESM2-LM	SAM0-UNICON	TaiESM1	UKESM1-0-LL
tas normalized bias	−0.18	−0.09	−0.21	−0.87	0.19	0.07	−0.11	−0.02	−0.3	0.25	−0.34	−0.2	−0.1
tas bias / snc bias	−0.35	−0.28	0.16	−0.62	−0.71	−0.58	0.09	−0.23	−0.16	−0.25	−0.18	−0.09	−0.17
tas bias / pr bias	0.03	0.09	0.07	0.05	−0.12	0.15	−0.24	−0.32	−0.1	−0.25	−0.03	−0.08	0.05
snc bias / pr bias	−0.01	0.11	0.09	0.08	0.19	−0.38	−0.09	0.15	−0.23	0.27	0.13	0.02	0.02
tas bias / elevation	−0.43	−0.16	−0.09	−0.63	−0.28	−0.52	−0.3	−0.21	−0.42	−0.05	−0.45	−0.34	−0.12
snc bias / elevation	0.5	0.47	0.32	0.56	0.41	0.56	0.22	0.24	0.44	0.29	0.48	0.39	0.49
pr bias / elevation	−0.27	−0.17	−0.49	−0.22	−0.15	−0.2	−0.16	0.05	−0.17	−0.17	−0.15	−0.2	−0.15

Historical trends analysis